

# Acetylcholinesterase-Positive Fiber Deafferentation and Cell Shrinkage in the Septohippocampal Pathway of Aged Amyloid Precursor Protein London Mutant Transgenic Mice

Francisca C. Bronfman, Dieder Moechars,<sup>1</sup>  
and Fred Van Leuven

*Experimental Genetics Group, Center for Human Genetics, Flemish Institute for Biotechnology, K. U. Leuven, Campus Gasthuisberg, B-3000 Leuven, Belgium*

Received February 3, 2000; accepted February 10, 2000

Several lines of evidence implicate a cholinergic deficit in Alzheimer's disease (AD). Transgenic mice that overexpress clinical mutants of the human amyloid precursor protein (APP) have been generated that recapitulate many aspects of AD. We now analyzed the cholinergic system in aged APP/London transgenic mice. The major finding was the reorganization of acetylcholinesterase-positive fibers within the hippocampus and the reduced size of cholinergic cells in the medial septum. The reduction of acetylcholinesterase-positive fibers in the subiculum together with increased fiber density in the CA1 and in the dentate gyrus suggests a synaptic sprouting compensatory mechanism within the hippocampus. In the cortex, amyloid plaques were associated with intense acetylcholinesterase activity and surrounded by dystrophic acetylcholinesterase-positive fibers. Nevertheless, the overall pattern of cholinergic innervation was unchanged. These results demonstrate that overexpression of APP/London caused, besides amyloid plaques in aged mouse brain, also cholinergic deafferentation and cholinergic cell shrinkage. © 2000 Academic Press

**Key Words:** Alzheimer's disease; transgenic mice models; cholinergic system; aging; amyloid plaques.

## INTRODUCTION

Alzheimer's disease (AD) is the most common type of dementia (75%), manifesting as a severe deterioration of mental functions (Cummings & Kaufer, 1996). Familial AD patients are due to mutations in the amyloid precursor protein (APP) and in the presenilin genes. Most AD patients are sporadic cases (Pericak-Vance & Haines, 1995).

Postmortem AD brain is characterized by the presence of amyloid plaques, neurofibrillary tangles, synaptic loss and cell loss, and neurotransmitter derangement. The amyloid plaques are extracellular deposits of A $\beta$  peptide, a proteolytic fragment of APP (Haass &

Selkoe, 1993). Neurofibrillary tangles are intracellular aggregates formed by a hyperphosphorylated form of the microtubule-associated protein tau (Goedert, 1993). A consistent neurotransmitter derangement in AD is the cholinergic deficit (Geula & Mesulam, 1994; Procter *et al.*, 1996). The cholinergic problem continues to attract interest because its magnitude correlates with the severity of dementia (Perry *et al.*, 1978; Bierer *et al.*, 1995). Drugs that target the cholinergic system are at this moment the main type of drugs available to treat the symptoms of AD (Parnetti *et al.*, 1997; Francis *et al.*, 1999).

Several transgenic mice models overexpressing APP and its clinical mutants have been generated which recapitulate aspects of AD. Amyloid plaques and neuritic changes have been obtained in addition to astrogliosis, microglial activation and increased tau phos-

<sup>1</sup> Present address: Department of Functional Genomics, Janssen Research Foundation, Beerse, Belgium.



phorylation (Higgins *et al.*, 1995; Games *et al.*, 1995; Hsiao *et al.*, 1996; Stürchler-Pierrat *et al.*, 1998; Frautschy *et al.*, 1998; Moechars *et al.*, 1999). Neuronal loss has been identified in one of these models (Calhoun *et al.*, 1998) but not in others (Irizarry *et al.*, 1996a,b). Disruption of neuronal circuits was reported to be independent of amyloid plaques (Hsia *et al.*, 1999), which are also not a prerequisite for early cognitive defects (Moechars *et al.*, 1999). Thus, these are good models to study which of the alterations observed in AD are related to the process of amyloid formation (Price *et al.*, 1998).

In one APP transgenic mouse model, amyloid plaques colocalized with acetylcholinesterase and dystrophic cholinergic neurites (Stürchler-Pierrat *et al.*, 1998). In a double transgenic mouse, overexpressing APP and presenilin 1 clinical mutants, a reduction in the size of cholinergic boutons was observed in the hippocampus and cortex without alteration of the size of cholinergic neurons (Wong *et al.*, 1999). In postmortem brain of AD patients the cholinergic deficit has been reported to correlate with the density of amyloid plaques (Perry *et al.*, 1978; Geula & Mesulam, 1994), while a more recent study showed that the cholinergic deficit is better correlated with tangle density (Geula *et al.*, 1998).

An extensive analysis of the cholinergic system in aged transgenic mice that overexpress APP and develop amyloid plaques has not been addressed. Recently, we have generated and characterized transgenic mice that develop early and late phenotypic traits. These APP/London transgenic mice showed as early as 3- to 4-month robust changes in behavior, i.e., hyperactivity, anxiety, aggression and neophobia, and cognitive deficits measured by Morris water maze test and reduced long-term potentiation (Moechars *et al.*, 1998, 1999). Amyloid plaque deposition was a late process (>12 months) (Moechars *et al.*, 1999). We now analyzed whether a cholinergic deficit was present in aged and young APP/London transgenic mice. Different aspects of the cholinergic system that are affected in AD (McGeer *et al.*, 1984; Vogels *et al.*, 1990; Bissette *et al.*, 1996; Rodríguez-Puertas *et al.*, 1997; Arendt *et al.*, 1992) were studied: the extent of cholinergic fiber innervation in the cortex and hippocampus by quantitative acetylcholinesterase (AChE) histochemistry; the AChE and choline acetyltransferase (ChAT) activity levels in different areas of the brain, in addition to the analysis of the molecular forms of AChE; the cholinergic cell number and gross morphology by immunohistochemistry against ChAT. Finally, we included the study of high affinity choline trans-

porter (HACHT), a presynaptic marker and the muscarinic type 1 receptor (M1) a postsynaptic marker, in young APP/London transgenic mice, to address in more detail whether the overexpression of the London mutant form of APP disrupted the cholinergic synapse.

## MATERIALS AND METHODS

### Materials

The polyclonal antibody against ChAT was purchased from Chemicon International (Tremula, CA) (AB144P). FCA18 polyclonal antibody against amyloid peptide was used as described (Barelli *et al.*, 1997). Secondary antibodies conjugated with biotin were purchased (DAKO, Glostrup, Denmark). [<sup>3</sup>H]Acetyl coenzyme A, [<sup>3</sup>H]pirenzepine, and [<sup>3</sup>H]hemicholinium-3 were purchased from NEN, Life Science Products, Inc. (Boston, MA). Atropine, hemicholinium-3, tetraisopropylpyro-phosphoramidate (Iso-OMPA), 1,5-bis (4-allyldimethylammoniumphenyl) pentan-3-one dibromide (Bw284c51), choline iodide, acetyl coenzyme A, hemicholinium-3, acetylthiocholine iodide, tetraphenylborate, and 3-heptanone were purchased by Sigma (St. Louis, MO).

### Mice

Transgenic mice carrying the amyloid precursor protein London (695 isoform) mutation (V642I) were generated as described (Moechars *et al.*, 1996, 1999). All mice were identically housed in a temperature and humidity controlled vivarium, kept on a 12-h dark-light cycle (light on 7:00 EST), with free access to food and water. Aged APP/London between 17–22 months and age-matched nontransgenic mice (FVB wild type) and young APP/London between 4–6 months and age-matched nontransgenic mice were processed simultaneously for all the assays performed.

### Histology

The brains of six APP/London and six nontransgenic mice (17–22 months) were fixed by cardiac perfusion under deep anesthesia with 5 ml saline followed by 20 ml cold fixative (4% paraformaldehyde, in 0.1 M phosphate buffer, pH 7.4) and then postfixed for 24 h in the same solution at 4°C. Fixed brains were stored for another 24 h in 0.1 M phosphate buffer (pH 7.4), 150 mM NaCl at 4°C. From each brain, serial

vibratome sections were obtained. The free-floating coronal sections (40  $\mu\text{m}$ ) were collected in 0.1 M phosphate buffer and processed for amyloid immunostaining, thioflavine S staining choline acetyltransferase (ChAT) immunostaining, and acetylcholinesterase (AChE) histochemistry.

**Immunohistochemistry.** ChAT immunostaining was performed as follows: (i) 30-min incubation at 4°C with 0.4% Triton X-100 in 0.1 M Tris-HCl, 150 mM NaCl, pH 7.4 (TBS); (ii) 1-h incubation at 4°C with 0.1% Triton X-100, 5% rabbit serum, 5% albumin in TBS; (iii) 48-h incubation at 4°C with antibody to ChAT (AB144P) diluted 1:500 in 0.1% Triton X-100, 5% rabbit serum in TBS; (iv) 1-h incubation at room temperature with biotin-conjugated rabbit anti-goat IgG (diluted 1:300 in 0.1% Triton X-100, 5% nonimmune rabbit serum in TBS); (v) 1-h incubation with avidin conjugated to peroxidase (ABC, DAKO, Denmark), followed by visualization of peroxidase activity with diaminobenzidine (1 mg/ml), 2% ammonium nickel sulfate, and H<sub>2</sub>O<sub>2</sub> (0.01%) in 50 mM Tris-HCl (pH 7.6). Amyloid immunostaining was performed as follows: (i) 1-h incubation at room temperature with 0.2% Triton X-100 and 10% goat serum in TBS; (ii) 48-h incubation at 4°C with FCA18 antibody to A $\beta$  peptide (diluted 1:500 in 0.2% Triton X-100 and 10% goat serum in TBS); (iii) 1-h incubation at room temperature with biotin-conjugated goat anti-rabbit IgG (diluted 1:300 in 0.1% Triton X-100, 5% nonimmune goat serum in TBS); (iv) 1-h incubation with avidin conjugated to peroxidase (ABC, DAKO, Denmark), followed by visualization of peroxidase activity with diaminobenzidine (1 mg/ml), and H<sub>2</sub>O<sub>2</sub> (0.01%) in 50 mM Tris-HCl (pH 7.6).

**Acetylcholinesterase (AChE) enzyme-histochemistry.** Serial coronal vibratome sections (40  $\mu\text{m}$ ) were collected in 0.1 M phosphate buffer (pH 7.4) and were incubated, as free-floating sections for staining (Karnovsky & Roots, 1964) modified as follows (Tago *et al.*, 1986): (i) incubation for 30 min at room temperature with 0.3% H<sub>2</sub>O<sub>2</sub> in 50 mM Tris-HCl buffer (pH 7.6); (ii) incubation for 1 h at room temperature in 0.05 mg/ml acetylthiocholine iodide, 0.1 mM tetra-isopropyl-pyrophosphatamide, 0.05 mM potassium ferricyanide, 0.3 mM CuSO<sub>4</sub>, 0.5 mM sodium citrate, 65 mM sodium maleate (pH 6.0); (iii) 10-min incubation in 0.3% ammonium nickel sulfate, 0.04% diaminobenzidine, 50 mM Tris-HCl (pH 7.6), and ultimately H<sub>2</sub>O<sub>2</sub> to a final concentration of 0.03% was added and incubated for another 5 min.

## Morphometric Analysis

**Cholinergic cell counting.** Basal forebrain cholinergic neurons were defined from anatomical landmarks of the mouse brain atlas (Franklin & Paxinos, 1997). The anterior commissure, anterior, and the lateral ventricles defined the ventral border of the medial septum (MS). The meeting of the body of the corpus callosum at the midline marked the anterior boundary and the midline crossing of the anterior commissure and the appearance of the fornix marked the posterior boundary. Three 40- $\mu\text{m}$ -thick coronal sections were considered through the complete medial septum with a 120- $\mu\text{m}$  interval between each to avoid counting the same cell twice (coordinates from Bregma: 1.10 to 0.5 mm). The cholinergic cells of the horizontal limb of the diagonal band (DB) were defined as the group of immunopositive cells residing below the anterior commissure, anterior, and the anterior commissure, posterior. The appearance of the anterior commissure, posterior, marked the anterior boundary and the connection of the lateral ventricles marked the posterior boundary. Five 40- $\mu\text{m}$ -thick coronal sections were analyzed with 80  $\mu\text{m}$  of interval (Coordinates from Bregma: 0.38 to -0.34 mm). The cholinergic cells of the nucleus basalis magnocellularis (NBM) straddle the border between the lateral globus pallidus and the internal capsule. The anterior boundary was defined as the connection of lateral ventricles (coordinate from Bregma: -0.34 mm) and the posterior boundary was defined with the dorsal hippocampus (coordinates from Bregma: -1.34). Five 40- $\mu\text{m}$ -thick coronal sections were analyzed with 80- $\mu\text{m}$  interval. In each mouse the same number of sections and similar total distance for each nucleus were analyzed for cholinergic cell quantification to guaranty that similar volume of each nucleus was quantified.

For each section, immunopositive neuronal profiles were counted manually on photographs taken with a 10 $\times$  objective on a Zeiss IM35 inverted optic microscope. Only cells with a clear nucleus were measured and in cases when staining was too dark only cells with a clear neuronal morphology were considered. The final magnification of the photograph was four times the negative (10  $\times$  15 cm). This procedure allows clear visualization of cholinergic cells. The total area covered for each photograph was 670  $\times$  1000  $\mu\text{m}$ , enough to include all immunopositive cells of each cholinergic nucleus analyzed.

The total number of neuronal profiles counted in each set of three or five sections yielded the number of neurons per animal, corrected according to Abercrom-

bie (1946). In addition, ChAT immunopositive cells were counted on images digitized on a Leica DMR microscope (20× objective), equipped with a CCD video camera, and connected with a computerized image analysis system (AIS/C, Imaging Research, Canada). The image was incremented by 200% and using a viewing box, neurons were identified on the screen and counted. Two fields of  $665 \times 470 \mu\text{m}$  were considered for the analysis of the MS, one for the DB, and two for the NBM. Both procedures gave very comparable numbers of neuronal profiles.

**Size of cholinergic neurons.** A total of 100 neurons were assessed in each nucleus in each animal by measurement of cross-sectional area (a total of 600 neuronal profiles per genotype). Using objective 20×, fields of  $665 \times 470 \mu\text{m}$  were digitized and incremented by 400%. The image was processed with the detail extractor function that enhances the contrast and accentuated the edges of the neuronal profiles. The neuronal profiles were identified on screen and the cross sectional area ( $\mu\text{m}^2$ ) was calculated. The results are presented as the mean cross sectional area (neuronal size)  $\pm$  SEM.

**Fiber density.** The analytical imaging station operation system AIS/C was used to quantify fiber density (1.6× objective). The scan area function was used to define criteria (range of relative optical density) for automatic target detection.

Extent of cholinergic innervation was determined in three AChE stained sections, spaced at  $80 \mu\text{m}$  through the ventral hippocampus ( $-2.46$  to  $-2.80$  from Bregma, approx.). The CA1 field of hippocampus (CA1) the dentate gyrus (DG), the subiculum (S), and the entorhinal cortex (EC) were analyzed. The areas within the hippocampus were defined anatomically as defined in the mouse brain atlas (Franklin & Paxinos, 1997). The entorhinal cortex was defined as the region that included the entorhinal, perirhinal, and lateral entorhinal cortex as defined in the mouse brain atlas (Franklin & Paxinos, 1997). To measure the cholinergic innervation in the frontal cortex (FC), three AChE-stained sections spaced at  $80 \mu\text{m}$  through the striatum were analyzed ( $\sim 0.74$  from Bregma). The somatosensory cortex defined by the mouse brain atlas (Franklin & Paxinos, 1997) was the main structure labeled. A total of six areas were analyzed per mouse (from the left and right side of each section). The optical density measured in the corpus callosum was used as internal background density per mouse.

For the CA1 region the proportional area was also calculated. This is defined as the total area of the target pixels contained within the region of interest relative

to the total scan area. Six CA1 areas were analyzed per mice (digitized with a 20× objective lens) and six random fields ( $110 \times 85 \mu\text{m}$ ) were considered per CA1 region.

### Biochemical Assays

**Sample preparation.** Four APP/London and four age-matched nontransgenic mice were killed by cervical dislocation and brains were removed. The hippocampus and the cortex were carefully dissected, washed in 0.1 M phosphate buffer saline and 150 mM NaCl (pH 7.4), and weighed. The tissue (10% wt/vol) was homogenized in ice cold buffer A [50 mM Tris-HCl, pH. 7.4, 1.0 M NaCl, 2.5 mM EDTA, and 50 mM  $\text{MgCl}_2$  (pH 7.4)], containing a cocktail of proteinase inhibitors in a glass teflon homogenizer. The suspension was centrifuged at 150,000g at  $4^\circ\text{C}$  for 1 h to recover the salt-soluble (SS) fraction in a Beckman TLA 100.4 rotor. The pellet was reextracted with buffer A containing 1% Triton X-100 and was centrifuged at 30,000g at  $4^\circ\text{C}$  for 1 h to recover a Triton X-100-soluble (TS) fraction. This method allows the extraction of more than 90% of the total AChE enzymatic activity (Sberna *et al.*, 1998). The protein concentration was measured by the method of Bradford *et al.* (1976).

**AChE activity assay and analysis of molecular isoforms.** AChE activity was determined by the method of Ellman *et al.* (1961). Briefly,  $5 \mu\text{l}$  of sample was mixed with  $200 \mu\text{l}$  of reaction buffer (0.5 mM phosphate buffer, pH7.4, 0.02% DTNB, 0.02% acetylthiocholine, and 0.1 mM iso-OMPA) The activity of the enzyme was determined after 5 min of incubation at room temperature and stopped with Bw284c51, a potent AChE inhibitor. The optical density was measured at 405 nm (Victor multilabel counter, Wallac). AChE activity was expressed as relative units and standardized by the amounts of protein of the sample.

For the analysis of the AChE molecular isoforms, the frontal and parietal cortex were analyzed together mixing equal amount of both homogenates. Supernatant fractions (SS and TS fraction) were centrifuged at 150,000g in a continuous sucrose gradient (5–20% wt/vol) for 18 h at  $4^\circ\text{C}$  in a Beckman SW41 rotor. The gradients contained 50 mM Tris-HCl (pH 7.4), 0.5 M NaCl, and 50 mM  $\text{MgCl}_2$  with 0.5% (wt/vol) Brij 97 or 0.5% (wt/vol) Triton X-100. Enzymes of known sedimentation coefficient, alkaline phosphatase (6.1S), and catalase (11.4S) were used in the gradients as markers (Sberna *et al.*, 1998). Forty fractions were collected from the bottom of the gradients in a 96-well micro-

plate. A 100- $\mu$ l sample of each fraction of the gradient was used to determine AChE activity as described above, the optical density background was determined by measuring the enzymatic activity in 100  $\mu$ l of each fraction in the presence of Bw284c51.

**ChAT enzymatic activity assay.** ChAT activity was measured as described (Fonnum, 1975). Briefly, 5  $\mu$ l of tissue homogenate (the salt soluble and the triton soluble fraction were analyzed together mixing equal amounts of each supernatant) was added to 10  $\mu$ l reaction buffer [75 mM sodium phosphate, pH 7.4, 600 mM NaCl, 40 mM MgCl<sub>2</sub>, 0.1 mM Bw284c51, 0.05% bovine serum albumin, 10 mM choline iodide, and 0.3 mM [<sup>3</sup>H]acetyl-CoA (~40 mCi/mmol, performed with a mix of cold and hot acetyl-CoA)]. This mixture was then incubated for 30 min at 37°C. The reaction was stopped by the addition of 150  $\mu$ l of tetraphenylboron (75 mg/ml in 3-heptanone), gently mixed, and centrifuged. One hundred microliters of the organic top layer was removed and placed into scintillation vials. The levels of ChAT activity were determined by subtracting the cpm in the blank tubes (without tissue) from the cpm in the tubes with tissue. The activity was calculated as cpm/ $\mu$ g proteins/30 min. The ChAT activity levels of the brain regions analyzed in the transgenic mice were normalized as the percentage of the levels obtained in nontransgenic mice.

### Receptor Binding Assays

The high affinity choline transporter (HACHT) was labeled with [<sup>3</sup>H]hemicholinium-3. Assay of [<sup>3</sup>H]hemicholinium-3 binding sites was performed as described (Happe & Murrin, 1992). Serial frozen coronal brain sections (16  $\mu$ m) from the level of the genu of the corpus callosum to the level of the ventral hippocampus were mounted on glass-slides and used for binding studies. The slides were coated with polylysine to reduce the nonspecific binding of [<sup>3</sup>H]hemicholinium-3. The sections were air-dried and kept at -70°C until used. Sections were equilibrated at room temperature and incubated for 30 min in 50 mM glycine-glycine (pH 7.8), 200 mM NaCl, and six different concentrations ranging from 1.25 to 30 nM [<sup>3</sup>H]hemicholinium-3 (120 Ci/mmol). After washing twice for 2 min in cold buffer, followed by rinsing in cold water, the sections were air-dried and exposed to [<sup>3</sup>H]Hyperfilm (Amersham, UK) for 2 weeks. Nonspecific binding was determined by addition of 10  $\mu$ M hemicholinium-3 cold to the incubation mixture. Plastic embedded tritium standards ([<sup>3</sup>H]Micro-scale, activity levels, 3-110 nCi/mg, Amersham, UK) were coex-

posed with tissue section. Autoradiographic images from the sections were scanned and the optical density from the hippocampus, frontal cortex, entorhinal cortex, was quantified using the analytical imaging station AIS/C. The optical density value from the nonspecific binding was subtracted from each of the values. Each brain region was measured bilaterally in one section per concentration for each of the mice analyzed (4 APP/London and 4 age-matched nontransgenic mice, 4-6 months). The  $K_d$  and the  $B_{max}$  were obtained by Rosenthal (Scatchard) analysis of [<sup>3</sup>H]hemicholinium-3 binding curves (Rosenthal, 1967).

The muscarinic type 1 (M1) was labeled with [<sup>3</sup>H]pirenzepine. The Assay of [<sup>3</sup>H]pirenzepine binding sites in brain slices was performed as described (Aubert *et al.*, 1992). Frozen coronal brain sections (16  $\mu$ m) were mounted on gelatin coated slides, air-dried and kept at -70°C until use. The sections were equilibrated at room temperature for 15 min in Krebs buffer (120 mM NaCl, 1.2 mM MgSO<sub>4</sub>, 1.2 mM KH<sub>2</sub>P0<sub>4</sub>, 5.6 mM glucose, 25 mM NaHCO<sub>3</sub>, 2.5 mM CaCl<sub>2</sub>, 4.7 mM KCl, pH 7.4) and incubated for 1 h in fresh buffer containing 15 nM [<sup>3</sup>H]pirenzepine alone or with atropine (10  $\mu$ M) to determine nonspecific binding. Slides were rinsed three times in 50 mM Tris-HCl (pH 7.4) and once with cold water, before being air-dried and exposed to [<sup>3</sup>H]Hyperfilm (Amersham, UK) for 2 weeks. Images from CA1, CA3, dentate gyrus, frontal cortex, and entorhinal cortex were quantified by densitometric scanning using the analytical imaging station AIS/C. The optical density per brain area per mouse was the average from bilateral determinations on two sections per mouse (4 APP/London and 4 nontransgenic mice, 4-6 months).

Assay of [<sup>3</sup>H]pirenzepine binding sites in brain membranes was performed as described (Araujo *et al.*, 1990). Membrane fractions were prepared from mouse cortex and hippocampus by homogenization in Krebs buffer (120 mM NaCl, 1.2 mM MgSO<sub>4</sub>, 1.2 mM KH<sub>2</sub>P0<sub>4</sub>, 5.6 mM glucose, 25 mM NaHCO<sub>3</sub>, 2.5 mM CaCl<sub>2</sub>, 4.7 mM KCl, pH 7.4, and collected by centrifugation at 4°C, 20,000g, 20 min in a Beckman TLA 100.4 rotor). The pellets were washed twice by resuspending in fresh buffer and the final membrane pellet was resuspended in the same buffer. Aliquots equivalent to 100  $\mu$ g protein were incubated with specified concentrations of [<sup>3</sup>H]pirenzepine (70-87 Ci/mmol) for 1 h at room temperature in a final volume of 0.5 ml. Membranes were collected by rapid filtration under reduced pressure on glass-fiber filters (GF/C Whatmann) presoaked in 0.5% polyethyleneimine to reduce

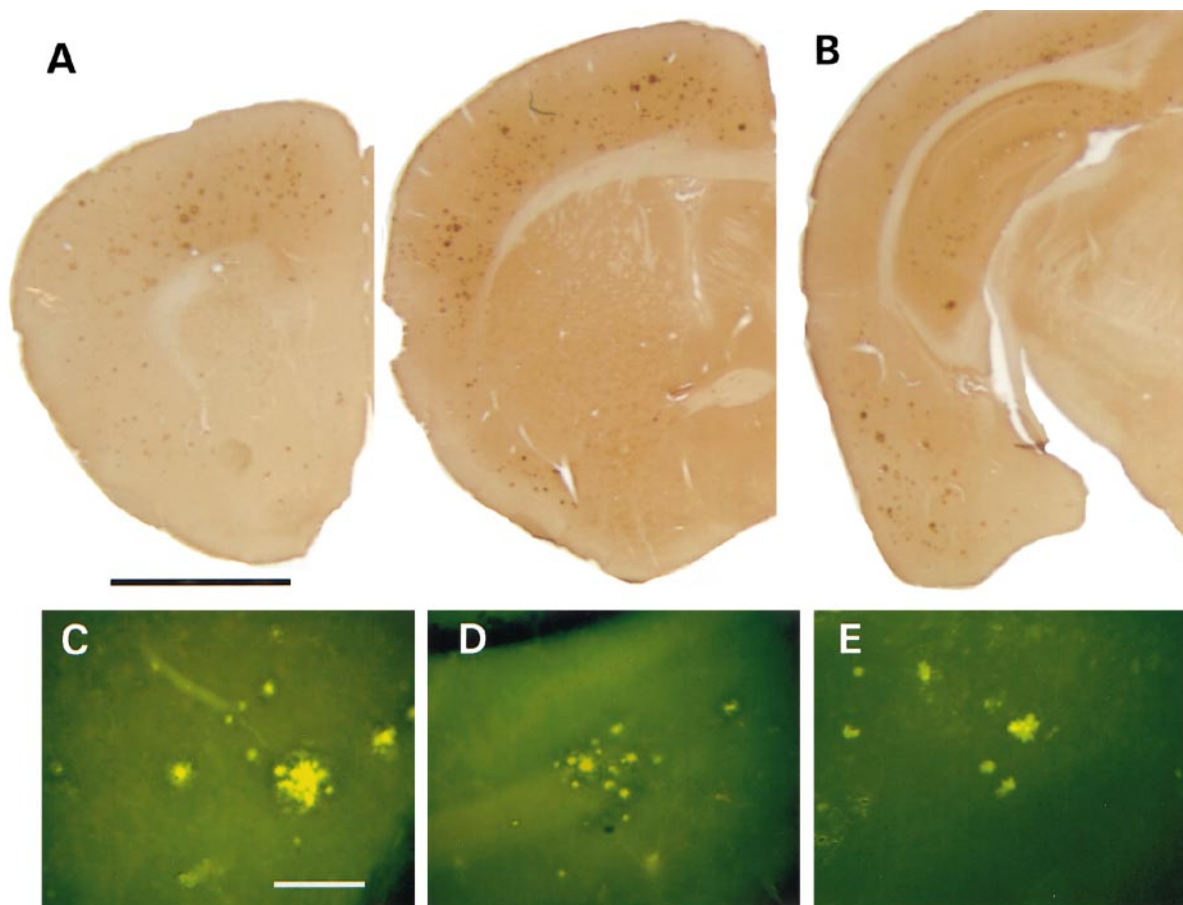


**FIG. 1.** Amyloid plaque distribution in aged APP/London transgenic mice (17–22 months). Coronal sections through the frontal cortex (A) and through the ventral hippocampus (B), stained with a polyclonal against the A $\beta$  peptide. Scale bar, 2 mm. (C, D, E) Thioflavine-S staining of amyloid plaques in the cortex, CA3, and subiculum, respectively, from the brain of aged APP/London transgenic mice. Scale bar, 100  $\mu$ m.

nonspecific binding. Filters were washed rapidly with ice-cold buffer and radioactivity counted. Specific binding was calculated as the difference in radioactivity bound in the presence and absence of 10  $\mu$ M atropine. Protein concentration was measured as described (Bradford, 1976).

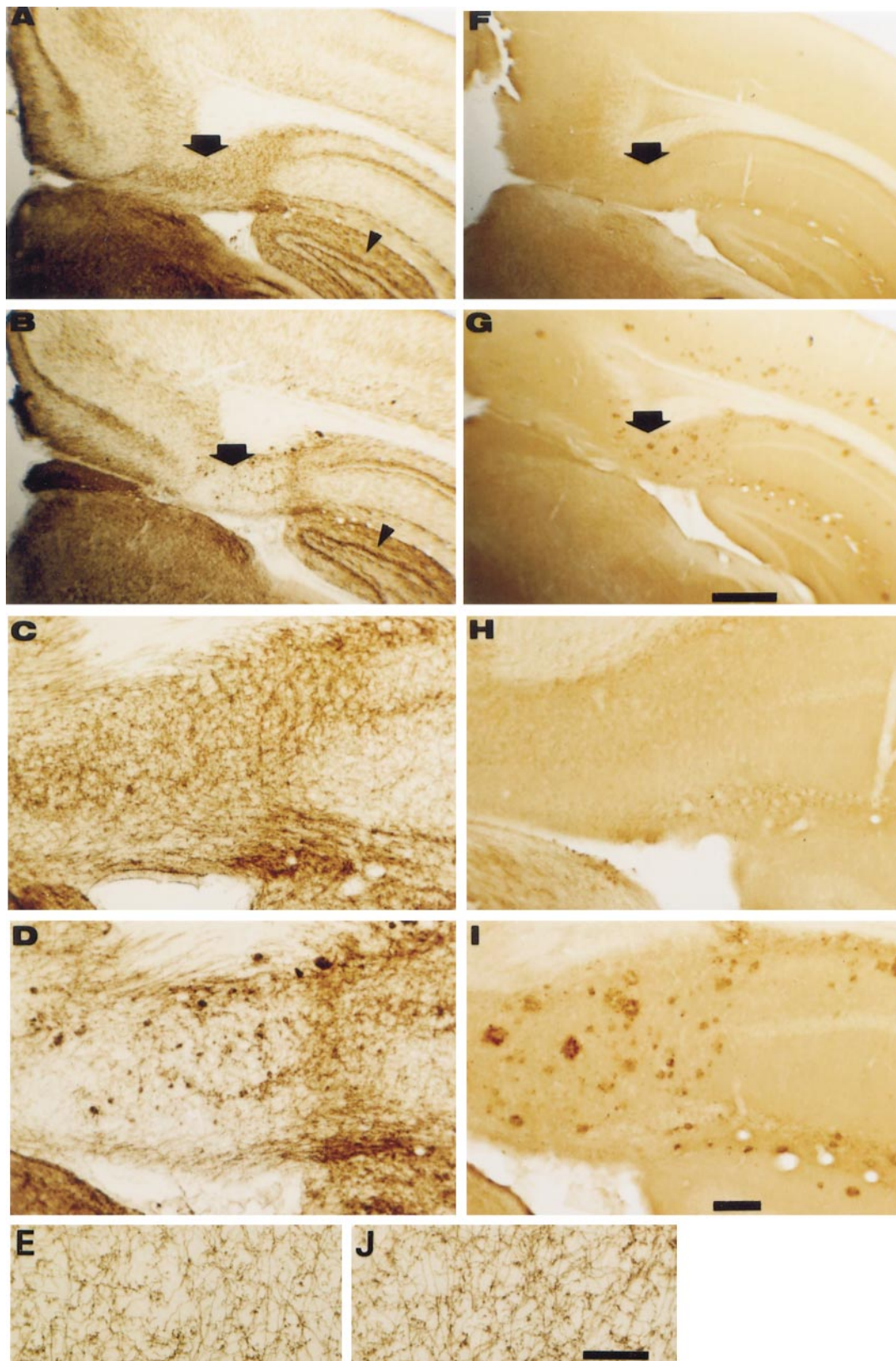
### Statistics

Student's two tailed *t* test was used to determine the statistical significance. The averages were expressed as the mean  $\pm$  SEM.

## RESULTS

In the APP/London transgenic mice amyloid plaque deposition is a late process that correlates with

increased levels of A $\beta$ (42) peptide (Moechars *et al.*, 1999). Amyloid plaques stained with a polyclonal against A $\beta$  peptide (Barelli *et al.*, 1997) were concentrated in the frontal cortex, mainly in layers IV–VI (Fig. 1A). More caudally through the ventral hippocampus, plaques were also evident in the entorhinal cortex, and amygdala. In the hippocampus, amyloid plaques were consistently present in the subiculum and more sporadically in other regions, i.e., the stratum radiatum, CA1 and CA3 regions (Figs. 1B, 2G, and 2I). Thioflavine-S staining of adjacent sections demonstrated the amyloid nature of the plaques in the cortex, in the CA3 region of the hippocampus and in the subiculum (Figs. 1C to 1E). Amyloid staining was never seen in old nontransgenic mice (Figs. 2F and 2H), demonstrating the specificity of the process and of the staining by the FCA 18 antibody (Barelli *et al.*, 1997; Moechars *et al.*, 1999).



We determined whether the presence of amyloid plaques in brain of aged APP/London transgenic mice affected the cholinergic system.

Cholinergic innervation was revealed by staining for acetylcholinesterase (AChE), a general marker for cholinergic fibers (Kitt *et al.*, 1994; Geula & Mesulam, 1994; Chen *et al.*, 1997). In the hippocampus, extensive cholinergic deafferentation became evident in the subiculum of aged APP/London mice (Figs. 2A to 2D). In the cortex, a subset of the amyloid plaques overlapped with strong AChE activity in adjacent sections (Figs. 3A to 3D, 3F to 3I), but the overall pattern of AChE-positive fibers remained essentially unaltered (Figs. 3E and 3J). In some amyloid plaques the intense AChE activity appeared to be contained in the core (Figs. 3C and 3D, 3H and 3I), while around most plaques AChE-positive fibers appeared distorted (Fig. 3G). Enlarged AChE-positive neurites overlapped with the amyloid plaques (Figs. 3C and 3D, 3H and 3I). When a specific acetylcholinesterase inhibitor (Bw284c51) was added to the AChE reaction buffer, AChE-positive fibers and AChE activity associated with amyloid plaques were not observed (data not shown).

Quantitative analysis of the AChE staining in the hippocampus demonstrated extensive cholinergic deafferentation of the subiculum, i.e., a 60% reduction in AChE activity ( $P < 0.01$ ) (Fig. 4A). A small increase (20%) in AChE activity was found in DG and CA1 ( $P < 0.05$  and  $P < 0.01$ , respectively) (Figs. 2A and 2B, 2E and 2J, and 4A).

We further analyzed the CA1 region of the hippocampus, because it allows clear visualization of the AChE positive fibers. An increased proportional scan area was measured in the CA1 (Fig. 4B), indicating that the increase in AChE activity was due to increased fiber density. Quantitative analysis of the cortex demonstrated no difference in AChE activity, neither in the frontal nor in the entorhinal cortex despite extensive amyloidosis (Figs. 3A and 3B).

To analyze if increased AChE activity in the amyloid plaques was associated with overall increased AChE activity levels or with an alteration in AChE molecular isoforms; we analyzed these parameters in

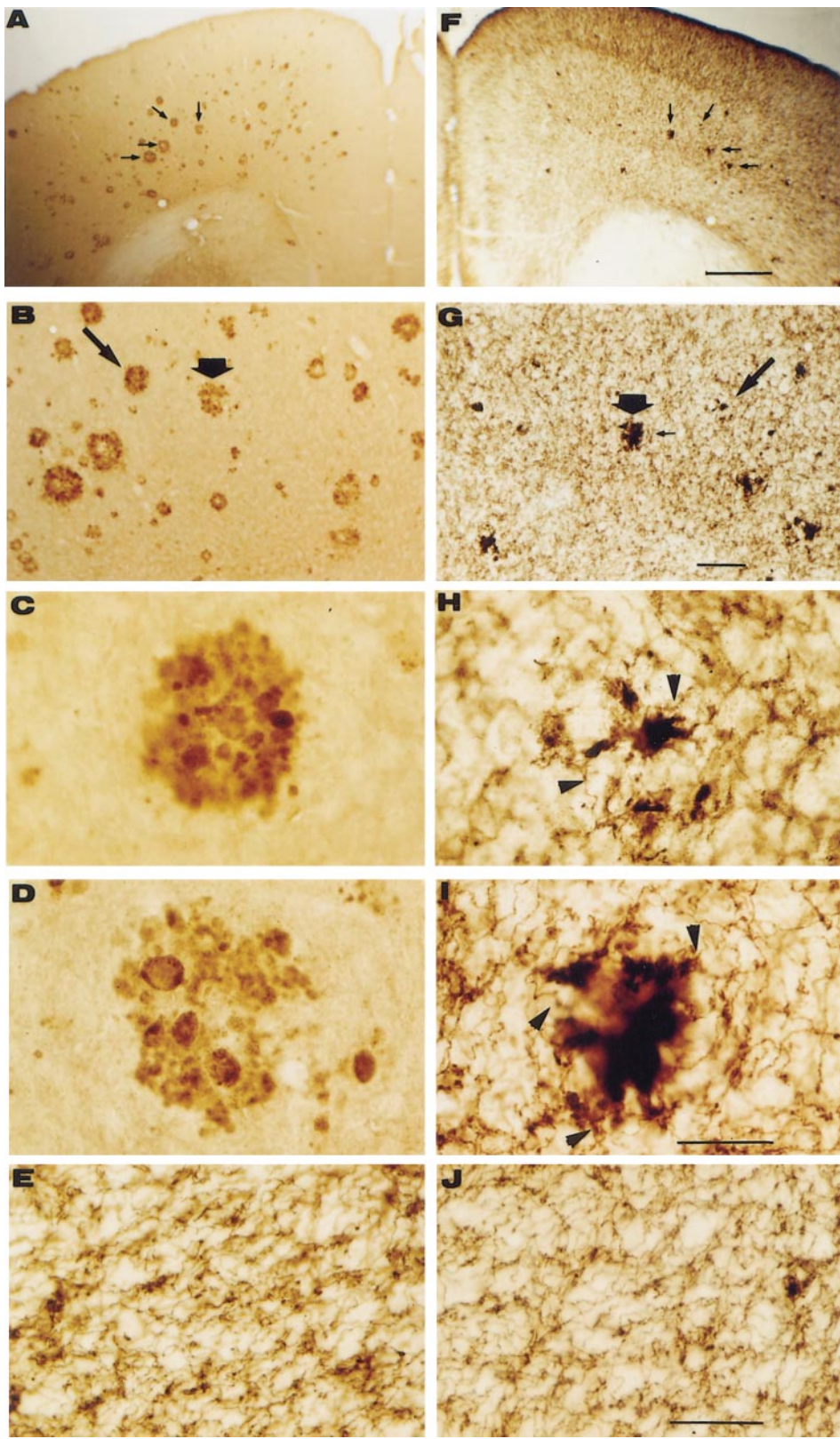
the hippocampus and the frontal and the parietal cortex. No changes in total AChE activity were found in any of the regions analyzed, neither in the triton soluble fraction (Fig. 5A) nor in the salt soluble fraction (Fig. 5B). Also no changes in the molecular isoforms of AChE were observed (Fig. 5C).

The cholinergic cells in mammalian brain are located in several nuclei of the basal forebrain and are defined as ChAT immunoreactive (IR) neurons. Many of these neurons do not have clear boundaries and are intermingled with non-cholinergic cells (Geula & Mesulam, 1994; Dutar *et al.*, 1995). The more rostral of these nuclei, the medial septum, sends projections to the hippocampus, dentate gyrus and subiculum (Dutar *et al.*, 1995). More caudally, the horizontal limb of the diagonal band of Broca and the nucleus basalis magnocellularis (nucleus basal of Meynert in primates and humans) send projections to the entire cortical mantle and the amygdala (Geula & Mesulam, 1994). The gross morphology and the cholinergic cell number was measured after ChAT immunohistochemistry on serial sections from the basal forebrain of aged APP/London transgenic mice and age matched nontransgenic mice. In the medial septum of aged APP/London transgenic mice the cholinergic cells were reduced in size compared to aged matched nontransgenic mice ( $P < 0.05$ ) (Figs. 6A, 6C, and 7A). The morphology of cholinergic cells in DB and NBM was conserved (Figs. 6B, 6D, and 7A). Quantitative analysis of the number of cholinergic neurons revealed no change in any of the nuclei analyzed (Fig. 7B). ChAT activity level, determined in the target regions for cholinergic neurons, was increased in the hippocampus ( $P < 0.05$ ) but not in the frontal and parietal cortex (Fig. 7C).

All the parameters already analyzed in aged APP/London transgenic mice were also evaluated in young APP/London transgenic mice, but none of the parameters were altered (data not shown).

Finally, we studied the high affinity choline transporter as a presynaptic marker, and the M1 receptor as a postsynaptic marker of cholinergic synapses, in young APP/London transgenic mice using specific receptor binding assays. No differences were found in

**FIG. 2.** Cholinergic fiber reorganization in the hippocampus of aged APP/London transgenic mice. Partial view of the ventral hippocampus following AChE histochemistry (A, B) and A $\beta$ -peptide immunostaining (F, G) of aged FVB (A, F) and APP/London transgenic mice (B, G). The biggest arrow indicates the subiculum and the smallest one indicates the dentate gyrus. Scale bar, 50  $\mu$ m. Higher magnification of the subiculum region following AChE histochemistry (C, D) and A $\beta$ -peptide immunostaining (H, I) of aged FVB (C, H) and APP/London transgenic mice (D, I). Scale bar, 10  $\mu$ m. The fiber density in the CA1 field of the hippocampus is increased in aged APP London transgenic mice (J) compared with nontransgenic mice (E). Scale bar, 7  $\mu$ m.



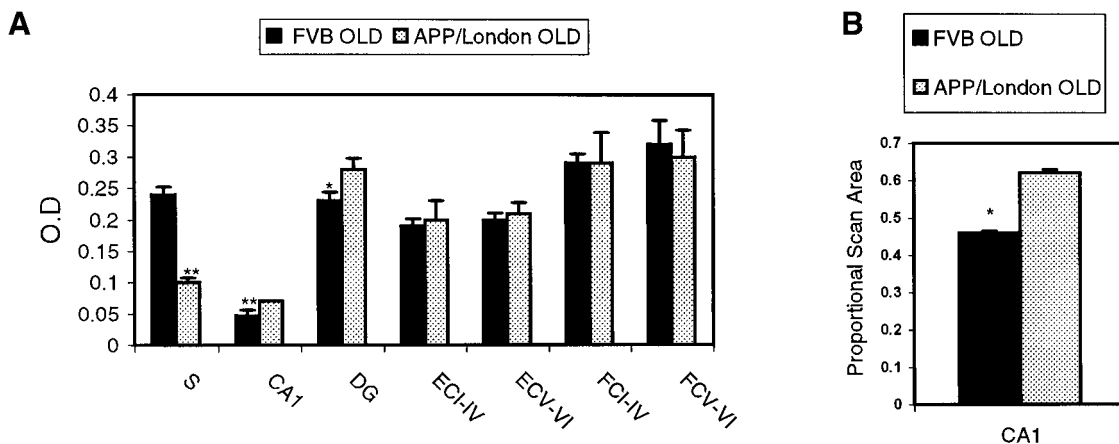


**FIG. 4.** Quantitative analysis of cholinergic fibers in different areas of age-matched nontransgenic and APP/London transgenic mice brain. (A) Optical density (O.D., relative units) of cholinergic fibers stained by AChE histochemistry in the subiculum (S), CA1 field of the hippocampus (CA1), dentate gyrus (DG), entorhinal cortex layer I to IV (EC I-IV), entorhinal cortex layer V and VI (EC V-VI), frontal cortex layers I to IV (FC I-IV), frontal cortex layers V and VI (FC V-VI), from FVB old (black bars) and APP/London transgenic mice (grey bars). (B) Proportional scan area (defined as the total area of the target grains contained within the region of interest relative to the total scan area) in the CA1 field of the hippocampus (CA1) from aged FVB (black bar) and APP/London transgenic mice (grey bar). Mean  $\pm$  SEM. \*Denotes a significant difference  $P < 0.05$ . \*\*Denotes a significant difference ( $P < 0.01$ ). Student's *t* test.

the distribution (Fig. 8A), the dissociation constant ( $K_d$ ) or maximum binding sites ( $B_{max}$ ) of the HACHT. The  $K_d$  values for nontransgenic mice were  $3.1 \pm 0.65$ ,  $2.1 \pm 0.28$ , and  $3.0 \pm 0.5$  (nM) in the hippocampus, frontal cortex, and parietal cortex, respectively, and the  $B_{max}$  values were  $45 \pm 7$ ,  $27 \pm 5$ ,  $33 \pm 3$  (fmol/mg tissue), in the hippocampus, frontal cortex and parietal cortex respectively. No alterations were found in the distribution, in the levels and binding parameters of the M1 receptor (Figs. 8B and 8C, and data not shown). This indicates that the cholinergic synapses were fully functional in young APP/London transgenic mice.

## DISCUSSION

We have undertaken an extensive comparative analysis of the cholinergic system in transgenic mice that

overexpress APP. The principal objective was to investigate the effects of the overexpression of APP London mutation and the presence of amyloid plaques on the status of the basal forebrain cholinergic system in young and aged mouse brain.

The major finding was an extensive AChE-positive fiber depletion of the subiculum, together with a reduction of the cholinergic cell size in the medial septum, demonstrating a prominent alteration in the septohippocampal pathway in these APP/London transgenic mice. Unexpectedly, we observed increased AChE levels in CA1 and DG within the hippocampal formation, together with increased ChAT activity levels. In the cortex, AChE activity was colocalized with the core of amyloid plaques and with enlarged cholinergic neurites. Nevertheless, the pattern of AChE-positive fiber innervation was conserved in the cortex and no changes in the activity levels or alterations in the molecular AChE

**FIG. 3.** Overlapping of amyloid plaques with AChE activity and cholinergic dystrophic neurites in aged APP/London transgenic mice brain. (A, F) Frontal cortex following  $A\beta$  peptide immunostaining (A) and AChE histochemistry (F). The arrows indicate 4 amyloid plaques (A) that overlap with 4 spots of AChE activity (F). Scale bar, 400  $\mu$ m. (B, G) Higher magnification of A (B) and of F (G). The biggest and the thickest arrows indicate the exactly amyloid aggregate (B) that overlap with accumulates of AChE activity (G). The smallest arrow indicates the local cholinergic fiber distortion induced by the presence of the plaque. Scale bar, 50  $\mu$ m. (C, H) Higher magnification of an amyloid plaque (C) indicated by the biggest arrow in B. An intense accumulation of AChE is apparent in the core of the amyloid plaque (H). The arrows indicate dystrophic neurites. (D, I) Higher magnification of an amyloid plaque (D) indicated by the thickest arrow in B. An intense accumulation of AChE colocalize with the amyloid plaque (I). The arrows indicate dystrophic neurites. C,H,D,I, scale bar, 50  $\mu$ m. (E, J) Higher magnification of the layer VI of the frontal cortex demonstrating that there is a conserved cholinergic innervation in age-matched nontransgenic mice (E) and APP/London transgenic mice (J). Scale bar, 50  $\mu$ m.

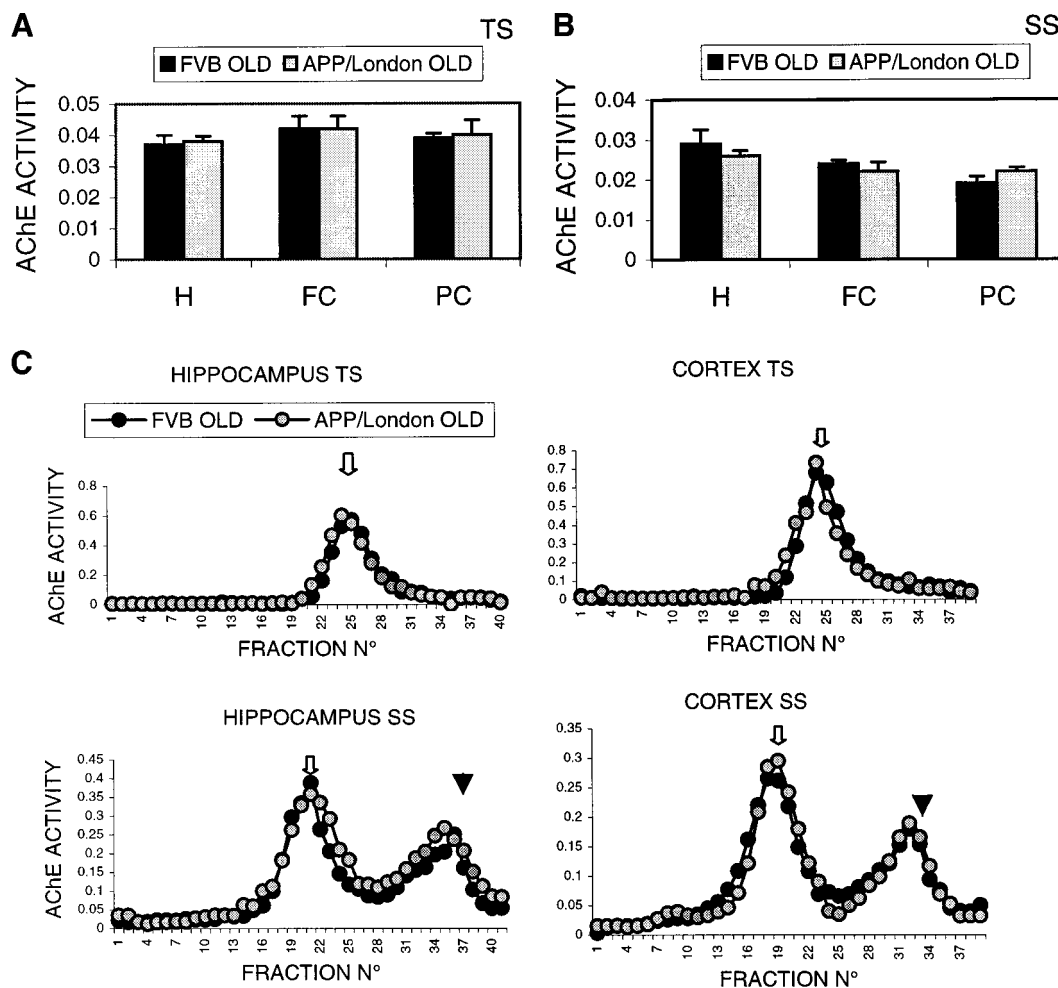


**FIG. 5.** AChE activity levels and molecular isoforms of hippocampus (H), frontal cortex (FC), and parietal cortex (PC) of age-matched nontransgenic and old APP/London transgenic mice brain. AChE activity (relative units) in the triton soluble fraction (TS) (A), and in the salt soluble fraction (SS) (B), of FVB old (black bars) and APP/London old (gray bars). AChE molecular isoforms (C) in the triton soluble fraction (TS) and salt soluble fraction (SS) in the hippocampus and cortex of FVB old (black circles) and APP/London old mice brain (gray circles). AChE activity corresponds to optical density (405 nm) standardized by proteins. Equal amount of proteins from the SS and TS homogenates was loaded at the top of the gradients to compare the different AChE isoforms from aged FVB and APP/London transgenic mice. The white arrow indicates the sedimentation of catalase, (G4 isoform), and the black arrow indicates the sedimentation of alkaline phosphatase, (G1 isoform).

isoforms were observed. In young APP/London transgenic mice no alterations were found in any of the parameters analyzed. In old APP/London transgenic mice, amyloid plaques in the brain contained or colocalized with intact AChE activity and with overlapping dystrophic cholinergic fibers, also observed in AD patients and in another strain of APP mutant transgenic mice (Morán *et al.*, 1984; Stürchler-Pierrat *et al.*, 1997). We demonstrated that this AChE activity increment in the plaques was not associated with overall increased AChE levels or

with altered molecular isoforms of AChE in the hippocampus or the cortex. Mice that overexpress the C-terminal fragment of APP have increased activity of a monomeric form of AChE (Sberna *et al.*, 1998), an effect that was not evident from our analysis of APP/London transgenic mice.

We observed before that AChE activity and an amyloid bearing fragment of APP increased in parallel in response to differentiation in a neuronal cell line, suggesting a common cellular regulation (Bronfman *et al.*, 1996). Signals, triggered by the close association of

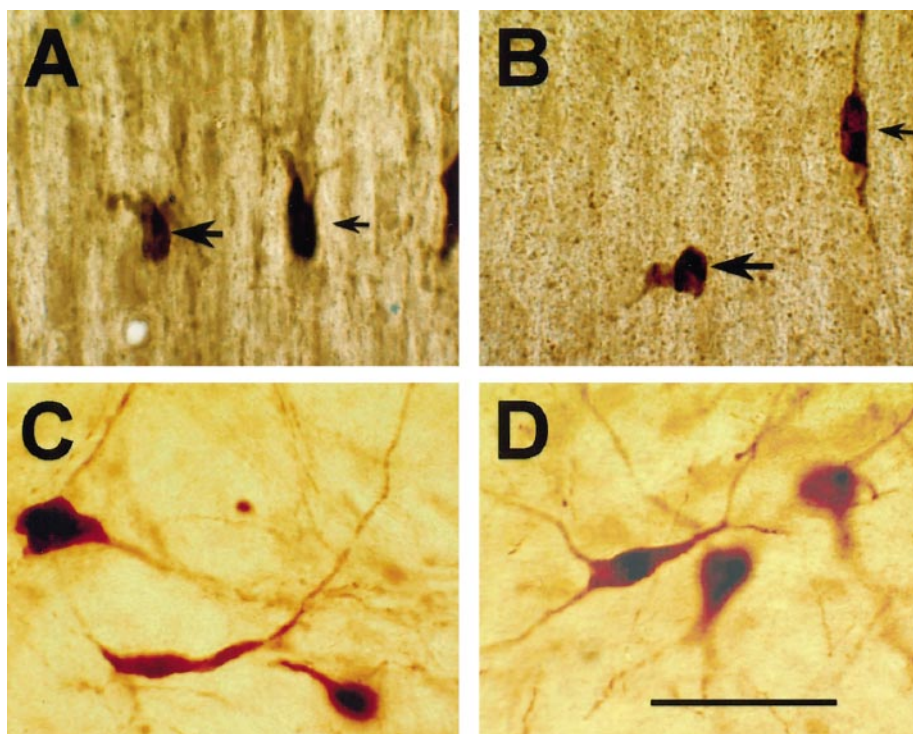


**FIG. 6.** ChAT-IR neurons in the medial septum (MS) and nucleus basalis magnocellularis (NBM) of age-matched nontransgenic and old APP/London transgenic mice brain. (A, C) ChAT-IR neurons in the MS, A, and in the NBM, C, from aged nontransgenic mice. A, the small arrow indicates a cell of  $131 \mu\text{m}^2$ , the big arrow indicates a cell of  $135 \mu\text{m}^2$ . (B, D) ChAT-IR neurons in the MS, B, and in the NBM; D, from aged APP/London transgenic mice. (B) The small arrow indicates a cell of  $89 \mu\text{m}^2$ , the big arrow indicates a cell of  $112 \mu\text{m}^2$ . The size of cholinergic neurons in the medial septum of aged APP/London transgenic mice appeared smaller compared with aged nontransgenic mice (indicated by the arrows). Scale bar,  $50 \mu\text{m}$ .

neurons with amyloid plaques could therefore induce the increased expression of AChE locally. Enlarged cholinergic neurites surrounding the plaques are the most likely source of the increased local AChE activity in the plaques.

It has been hypothesized that AChE might participate in the process of amyloid formation by inducing or contributing to the process of aggregation of amyloid peptides (Inestrosa *et al.*, 1996; Alvarez *et al.*, 1998) similar to ApoE (Bales *et al.*, 1997). In AD patients, the association of AChE activity with amyloid plaques was determined postmortem in the brain, when the cholinergic system is already completely devastated (Morán *et al.*, 1984). The results presented here demonstrate that this association is evident, even in the absence of a generalized or even minor cholinergic deficit in the cortex of APP London transgenic mice, making this an interesting model for this aspect of cholinergic pathology.

The subiculum is a predilected pathological area in AD brain, cholinergic fibers are reduced in this area of

AD patients (Flood, 1991; Ransmayr *et al.*, 1989). The subiculum is the primary output structure of the hippocampal formation and it plays a major role in processing spatial information and spatial memory, as indicated by studies of lesions and of neuronal recording (Schenk & Morris, 1985; Sharp & Green, 1994; Commins *et al.*, 1998, 1999).

It has been suggested that alterations in cholinergic neurons are a retrograde effect, secondary to primary cortical or hippocampal lesions (Cuellar & Sofroniew, 1994). Indeed, denervation of cholinergic neurons leads to cholinergic cell shrinkage in a cortical devascularization animal model without loss of neurons (Garofalo & Cuellar, 1994). When cholinergic neurons are disconnected from their target, they begin to degenerate because the source of trophic factors is lost (Williams *et al.*, 1986). A disconnection of septal neurons from a fraction of their target, i.e., subiculum, might explain why the cholinergic neurons of the medial septum were reduced in size in the APP/London transgenic mice.

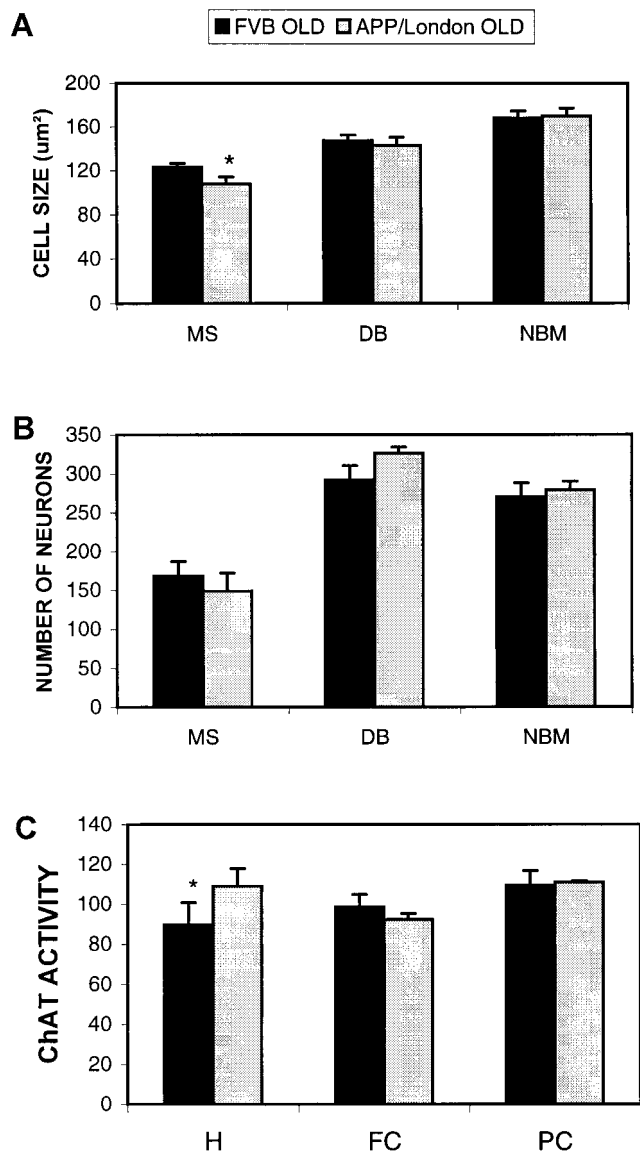


**FIG. 7.** Quantitative analysis of basal forebrain cholinergic neurons of age-matched nontransgenic (FVB) and old APP/London transgenic mice and ChAT activity levels in target regions. Size (A) and number (B) of ChAT-IR neurons in the medial septum (MS), horizontal limb of the diagonal band (DB), and nucleus basalis magnocellularis (NBM) of FVB old (black bars) and APP/London old (grey bars) transgenic mice brain. \*Denotes a significant difference in the size of ChAT-IR neurons in the medial septum of APP/London old transgenic mice compares with the control ( $P < 0.05$ ). Mean  $\pm$  SEM. Student's *t* test. (C) ChAT activity levels of FVB old (black bars) and APP/London old (grey bars) (expressed as percentage of the control). An increased ChAT activity appeared obvious in the hippocampus of aged APP London transgenic mice. Mean  $\pm$  SEM. \*Denotes a significant difference ( $P < 0.05$ ). Student's *t* test.

We observed an increased cholinergic fiber density in CA1 and DG of the hippocampus, in addition to the overall increased ChAT activity in brain of aged APP/London transgenic mice. This increased ChAT activity was not due directly to overexpression of APP, because in young transgenic mice this effect was not observed. We believe that the ChAT increment could be due to the sprouting reaction observed by AChE histochemistry in the hippocampus of aged APP/London transgenic mice by AChE histochemistry. The regenerative capacity of the cholinergic system is mediated principally by nerve growth factor (NGF), as well as other growth factors (William *et al.*, 1986; Garofalo *et al.*, 1992; Garofalo & Cuello, 1994; Koliatsos *et al.*, 1994; Fagan *et al.*, 1997; Chen *et al.*, 1997). Increased NGF levels are induced by cholinergic damage (Hellweg *et al.*, 1997), which suggests a mechanism for the terminal sprouting observed in the APP/London transgenic mice.

The hippocampal circuitry in the brain of AD patients is capable of plastic responses along with the regenerative events (Geddes *et al.*, 1985), an idea that is supported by our results. Ultrastructural studies of affected pathological areas in AD brain, i.e., the entorhinal cortex, subiculum, and CA1 are being performed in these APP transgenic mice to define ultrastructural changes at synaptic level. The fact that neither the subiculum is altered to any extent or the medial septal neurons present atrophy in young APP/London transgenic mice demonstrated that this effect was mediated by aging and amyloid deposition.

Overall AChE activity was unchanged in the hippocampus, in contrast to the increased ChAT activity in the aged APP/London transgenic mice. It has been reported that ChAT activity is up-regulated more extensively than AChE activity in response to NGF in rodent models of cholinergic injury and repair paradigm (Willson & Hanin, 1995). A different level of response to the deafferentation process might be the reason for this result.

Others did not find morphological differences in the cholinergic basal forebrain, despite an extensive amyloidosis and cholinergic terminals alteration in the cortex and hippocampus of double transgenic mouse (Wong *et al.*, 1999). Only young mice were analyzed, and aging is known to be the major risk factor for neuronal injury (Jucher & Ingram, 1997).

Study of the HACHT activity study was performed because the high affinity transport of choline is the limiting step in the synthesis of acetylcholine (Happe & Murrin, 1993). The level of HACHT is regulated by the activity of the cholinergic terminal, therefore a

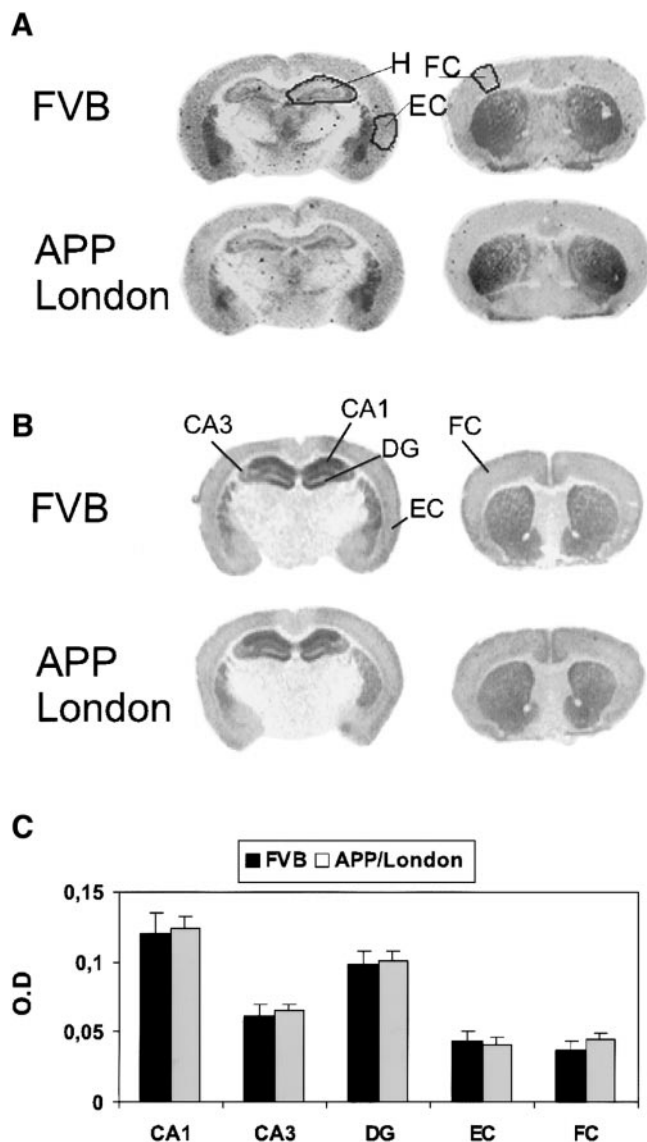


**FIG. 8.** Distribution of [ $^3\text{H}$ ]hemicholinium-3 and [ $^3\text{H}$ ]pirenzepine binding sites in brain sections of young nontransgenic and APP London transgenic mice. (A) Autoradiograms of [ $^3\text{H}$ ]hemicholinium-3 binding sites of age-matched nontransgenic (FVB) and young APP/London transgenic mice brain. A section through the hippocampus (left) and through the striatum (right) is shown for FVB and APP London transgenic mice brain (indicated at the left of the autoradiograms). The black line surrounds the regions utilized for quantitative determination of  $K_d$  (dissociation constant)  $B_{\text{max}}$  (maximal binding sites). Hippocampus (H), entorhinal cortex (EC), frontal cortex (FC). (B) Autoradiograms of [ $^3\text{H}$ ]pirenzepine binding sites of young FVB and APP London transgenic mice brain. A section through the hippocampus (left) and through the striatum (right) is shown for FVB and APP/London transgenic mice brain (indicated at the left of the sections). The black lines indicate the regions utilized for quantitative determination of relative optical density in C. CA1 field hippocampus (CA1), CA3 field hippocampus (CA3), dentate gyrus (DG), entorhinal cortex (EC), frontal cortex

dysfunctional cholinergic synapse could cause a reduction of the transporter activity without an obligatory loss of the terminal (Happe & Murrin, 1993). Our results demonstrated, however, that the cholinergic synapses were fully functional in young APP/London transgenic mice, even at the age when behavioral and cognitive deficits were evident (Moechars *et al.*, 1998, 1999).

Although pathological alterations were observed in the septohippocampal pathway in the aged APP/London transgenic mice, the cholinergic deficit as described in AD patients was not recapitulated completely. It is well known that the most affected cholinergic nucleus in AD patients is the nucleus basalis of Meynert (Whitehouse *et al.*, 1981). In our APP transgenic model the AChE-positive innervation was conserved in the cortex and no reduction in number or altered morphology was observed in the nucleus basalis magnocellularis, despite extensive presence of amyloid plaques in the neocortex. Possible reasons for this observation is that the amyloid plaques observed in the subiculum, the region of the hippocampus with consistent amyloid pathology, might have components that make them "more toxic" to cholinergic fibers or that these are more sensitive than in other areas of the brain. Characterization of amyloid plaques with different microglial markers and neuritic components is being performed to clarify this point. The outcome of our studies is important as it suggests that the cholinergic problems in AD are not an early or primary defect, corroborating another recent study (Davis *et al.*, 1999). These authors demonstrated that the neocortical cholinergic deficit was evident in very demented AD patients but was not apparent in individuals with mild AD. *In vivo* mapping of cholinergic terminals in AD patients demonstrated that they were reduced in AD, but not as extensively as suggested by postmortem studies (Kuhl *et al.*, 1996).

Alternatively, it remains possible that transgenic mice do not recapitulate this aspect of AD as an early phenotypic trait. These results implicate that none of the early phenotypic traits, including the learning and memory problems observed in young APP/London mice (Moechars *et al.*, 1999) are due to a cholinergic deficit.

(FC). (C) Quantification of [ $^3\text{H}$ ]pirenzepine binding to different brain areas (delineated in B) of coronal brain sections by densitometric scanning of the autoradiograms. O.D., optical density, (relative units). Mean  $\pm$  SEM. FVB (black bars) and APP/London transgenic mice (gray bars).

Our results also establish that the presence of human APP and of amyloid peptides deposited as amyloid plaques in old APP/London transgenic mice was not a sufficient trauma to affect the cholinergic system in a great extent. The likely reason for this finding is that the cholinergic deficit is more closely related to or even directly triggered by the pathological lesions involving protein tau, rather than by amyloid problems (Saper *et al.*, 1985; Terry *et al.*, 1996; Geula *et al.*, 1998). It has been described that basal forebrain cholinergic neurons show neurofibrillary degeneration as an early change (Saper *et al.*, 1985). The cortical load of paired helical filaments (PHF) is correlated with cholinergic dysfunction (Arendt *et al.*, 1999), although this relationship is not perfect (Geula *et al.*, 1998), suggesting additional factors in the cholinergic pathology. Up to now, it has been impossible to recapitulate tau pathology in transgenic mice, leaving this question open. Alternatively, the cholinergic deficit could be triggered by different quantitative and qualitative contributions of tau pathology and of amyloid formation. It is reasonable to propose that on the one hand the amyloid plaques are disturbing cholinergic innervation in the target region of cholinergic neurons and on the other hand that cholinergic neurons are being "injured" by neurofibrillary pathology. If this is the case, the present results obtained with old APP/London transgenic mice bearing amyloid plaques might represent the real contribution of amyloid plaques to the cholinergic deficit. This proposition is supported by the alteration of the cholinergic neuropil surrounding the amyloid plaques and by the reduction of cholinergic fibers in predilected pathological areas of AD brain as the subiculum (Ransmayr *et al.*, 1989; Flood *et al.*, 1991; Bobinski *et al.*, 1997). Evidently, the addition of neurofibrillary pathology to the current APP/London transgenic mouse model will undoubtedly settle these and other questions.

## ACKNOWLEDGMENTS

The authors gratefully acknowledge K. Spittaels, R. Lasrado, and J. Van Dorpe for carefully reading of the manuscript and I. Laenen for technical assistance. This investigation was supported by the Fonds voor Wetenschappelijk Onderzoek-Vlaanderen (FWO), by NFWO-Lotto, by the Interuniversity-network for Fundamental Research (IUAP), by the Special Biotechnology Program of the Flemish government (IWT/VLAB/COT-008), by a Flemish/Chilean bilateral scientific collaboration. F.C.B. received a doctoral fellowship from the Flemish community and from the K.U.Leuven.

## REFERENCES

- Abercrombie, M. (1946) Estimation of nuclear population from microtome sections. *Anat. Rec.* **94**, 239–247.
- Alvarez, A., Alarcón, R., Opazo, C., Campos, E. O., Munos, F. J., Calderón, F. H., Dajas, F., Gentry, M. K., Doctor, B. P., De Mello, F. G., & Inestrosa, N. C. (1998) Stable complexes involving acetylcholinesterase and amyloid- $\beta$ -peptide change the biochemical properties of the enzyme and increase the neurotoxicity of Alzheimer's fibrils. *J. Neurosci.* **18**, 3213–3223.
- Araujo, D. M., Lapchak, P. A., Meaney, M. J., Collier, B., & Quirion, R. (1990) Effects of aging on nicotinic and muscarinic autoreceptor function in the rat brain: Relationship to presynaptic cholinergic markers and binding sites. *J. Neurosci.* **10**, 3069–3078.
- Arendt, T., Brückner, M., Lange M., & Bigl, V. (1992) Changes in acetylcholinesterase and butyrylcholinesterase in Alzheimer's disease resemble embryonic development- A study of molecular forms. *Neurochem. Int.* **21**, 381–396.
- Arendt, T., Holzer, M., Gertz, H.-J., & Brückner M. K. (1999) Cortical load of PHF-tau in Alzheimer's disease is correlated with cholinergic dysfunction. *J. Neural. Transm.* **106**, 513–523.
- Aubert, I., Araujo, D. M., Cécyre, D., Robitaille, Y., Gauthier, S., & Quirion, R. (1992) Comparative alterations of nicotinic and muscarinic binding sites in Alzheimer's disease and Parkinson's disease. *J. Neurochem.* **58**, 529–541.
- Bales, K. R., Verina, T., Dodel, R. C., Du Y., Altstiel, L., Bender, M., Hyslop, P., Johnstones, E. M., Little, S. P., Cummins, D. J., Piccardo, P., Ghetti, B., & Paul, S. M. (1997) Lack of apolipoprotein E dramatically reduces amyloid beta-peptide deposition. *Nat. Genet.* **17**, 263–2634.
- Barelli, H., Lebeau, A., Vizzavona, J., Chevallier, N., Drout, C., Marambaud, P., Ancolio, K., Buxbaum, J. D., Khorkova, O., Heroux, J., Sahasrabudhe, S., Martinez, J., Warner, J. M., Mohr, M., & Checler, F. (1997) Characterization of new polyclonal antibodies specific for 40 and 42 amino acid-long amyloid beta peptides: Their use to examine the cell biology of presenilins and the immunohistochemistry of sporadic Alzheimer's disease and cerebral amyloid angiopathy cases. *Mol. Med.* **3**, 695–707.
- Bierer, L. M., Haroutunian, V., Gabriel, S., Knott, P. J., Carlin, L. S., Purohit, D. P., Perl, D. P., Schmeidler, J., Kanof, P., & Davis, K. L. (1995) Neurochemical correlates of dementia severity in Alzheimer's disease: relative importance of the cholinergic system. *J. Neurochem.* **64**, 749–760.
- Bissette, G., Seidler, F. J., Nemeroff, C. B., & Slotkin, T. A. (1996) High affinity choline transporter status in Alzheimer's disease tissue from rapid autopsy. *Ann. N. Y. Acad. Sci.* **777**, 197–204.
- Bobinski, M., Wegiel, J., Tarnawski, M., Bobinski, M., Reisberg, B., De Leon, M. J., Miller, D. G., & Wisniewski, H. M. (1997) Relationships between regional neuronal loss and neurofibrillary changes in the hippocampal formation and duration and severity of Alzheimer disease. *J. Neurophatol. Exp. Neurol.* **56**, 414–420.
- Bradford, M. M. (1976) A rapid and sensitive method for the quantification of micrograms quantities of protein utilizing the principle of protein dye binding. *Anal. Biochem.* **72**, 248–254.
- Bronfman, F. C., Fernandez, H. L., & Inestrosa, N. C. (1996) Amyloid precursor protein fragment and acetylcholinesterase increase with cell confluence and differentiation in a neuronal cell line. *Exp. Cell. Res.* **229**, 93–99.
- Calhoun, M. E., Wiederhold, K.-H., Abramowski, D., Phinney, A. L., Probst, A., Sturchler-Pierrat, C., Staufenbiel, M., Sommer, B., & Jucker, M. (1998) Neuron loss in APP transgenic mice. *Nature* **395**, 755–756.

- Chen, K. S., Nishimura, M. C., Armanini, M. P., Crowley, C., Spencer, S. D., & Phillips, H. S. (1997) Disruption of a single allele of the nerve growth factor gene results in atrophy of basal forebrain cholinergic neurons and memory deficits. *J. Neurosci.* **17**, 7288–7296.
- Commins, S., Anderton, M., Gigg, J., & O'Mara S. (1999) The effects of the single and multiple episodes of theta patterned or high frequency stimulation on synaptic transmission from hippocampal area CA1 to the subiculum in rats. *Neurosci. Lett.* **270**, 99–102.
- Commins, S., Gigg, J., Anderson, M., & O'Mara S. M. (1998) The projection from hippocampal area CA1 to the subiculum sustains long-term potentiation. *Neuroreport* **9**, 847–850.
- Cummings, J. L., & Kaufer, D. (1996) Neuropsychiatric aspects of Alzheimer's disease: The cholinergic hypothesis revisited. *Neurology* **47**, 876–883.
- Cuello, A. C., & Sofroniew, M. V. (1984) The anatomy of the CNS cholinergic neurons. *Trends Neurosci.* **7**, 74–78.
- Davis, K. L., Mohs, R. C., Marin, D., Purohit, D. P., Perl, D. P., Lantz, M., Austin, G., & Haroutunian, V. (1999) Cholinergic markers in elderly patients with early signs of Alzheimer's disease. *JAMA* **281**, 1401–1406.
- Dutar, P., Bassant, M. H., Senut, M. C., & Lamour, Y. (1995) The septohippocampal pathway: Structure and function of a central cholinergic system. *Physiol. Rev.* **75**, 393–427.
- Ellman, G. I., Courtney, K. D., Andres, V., & Featherstones, R. M. (1961) A new rapid colorimetric determination of cholinesterase activity. *Biochem. Pharmacol.* **7**, 88–95.
- Fagan, A. M., Suhr, S. T., Lucidi-Philippi, C. A., Peterson, D. A., Holtzman, D. M., & Gage, F. H. (1997) Endogenous FGF-2 is important for cholinergic sprouting in the denervated hippocampus. *J. Neurosci.* **17**, 2499–2511.
- Flood, D. G. (1991) Region-specific stability of dendritic extent in normal human aging and regression in Alzheimer's disease. II. *Subiculum. Brain. Res.* **540**, 83–95.
- Fonnum, F. (1974) A rapid radiochemical method for the determination of choline acetyl transferase. *J. Neurochem.* **24**, 407–409.
- Francis, P. T., Palmer, A. M., & Wilcock, G. (1999) The cholinergic hypothesis of Alzheimer's disease: A review of progress. *J. Neurol. Neurosurg. Psychiatry.* **66**, 137–147.
- Franklin, B. J., & Paxinos, G. (1997) *The Mouse Brain in Stereotaxic Coordinates*, 1st ed. Academic Press, San Diego.
- Frautschy S. A., Yang F., Irizarry, M., Hyman, B., Saido, T. C., Hsiao, K., & Cole, G. M. (1998) Microglial response to amyloid plaques in APPsw transgenic mice. *Am. J. Pathol.* **152**, 307–317.
- Games, D., Adams, D., Alessandrini, R., Barbour, R., & Zhao, J. (1995) Alzheimer-type neuropathology in transgenic mice overexpressing V717F b-amyloid precursor protein. *Nature* **373**, 523–526.
- Garofalo, L., & Cuello, A. C. (1994) Nerve growth factor and the monosialoganglioside GM1: Analogous and different *in vivo* effects on biochemical, morphological, and behavioral parameters of adult cortically lesioned rats. *Exp. Neurol.* **125**, 195–217.
- Garofalo, L., Ribeiro-Da-Silva, A., & Cuello, A. C. (1992) Nerve growth factor-induced synaptogenesis and hypertrophy of cortical cholinergic terminal. *Proc. Natl. Acad. Sci. USA* **89**, 2639–2642.
- Geddes, J. W., Monaghan, D. T., Cotman, C. W., Lott, I. T., Kim, R. C., & Chang Chui, H. (1985) Plasticity of hippocampal circuitry in Alzheimer's disease. *Science* **230**, 1179–1181.
- Geula, C., Mesulam, M. M., Saroff, D. M., & Wu, C. K. (1998) Relationship between plaques, tangles, and loss of cortical cholinergic fibers in Alzheimer disease. *J. Neuropathol. Exp. Neurol.* **57**, 63–75.
- Geula, C., & Mesulam, M. M. (1994) Cholinergic systems and related neuropathological predilection patterns in Alzheimer disease. In: *Alzheimer Disease* (R. D. Terry, R. Koltzman, and K. L. Bick, Eds.). Chap. 15, pp. 263–291. Raven Press, New York.
- Goedert, M. (1993) Tau protein and the neurofibrillary pathology of Alzheimer's disease. *Trends Neurosci.* **16**, 460–465.
- Haass, C., & Selkoe, D. (1993) Cellular processing of beta-amyloid precursor protein and the genesis of amyloid beta-peptide. *Cell* **75**, 1039–1042.
- Happe, H. K., & Murrin, L. C. (1992) Development of high-affinity choline transporter sites in rat forebrain: A quantitative autoradiography study with [<sup>3</sup>H]hemicholinium-3. *J. Comp. Neurol.* **321**, 591–611.
- Happe, H. K., & Murrin, L. C. (1993) High-affinity choline transporter sites: Use of [<sup>3</sup>H]hemicholinium-3 as a quantitative marker. *J. Neurochem.* **60**, 1191–1201.
- Hellweg, R., Humpel, C., Löwe, A., & Hörtnagl, H. (1997) Moderate lesion of the rat cholinergic septohippocampal pathway increases hippocampal nerve growth factor synthesis/evidence for long-term compensatory changes? *Mol. Brain Res.* **45**, 177–181.
- Higgins, L. S., Rodems, J. M., Quon, C. D., & Cordell, B. (1995) Early Alzheimer disease-like histopathology increases in frequency with age in mice transgenic for  $\beta$ -APP751. *Proc. Natl. Acad. Sci. USA* **92**, 4402–4406.
- Hsia, A. Y., Masliah, E., McConlogue L., Gui-qiu, Y., Tatsuno, G., Hu, K., Kholodenko, D., Malenka, R. C., Nicoll, R. A., & Mucke, L. (1999) Plaque-independent disruption of neural circuits in Alzheimer's disease mouse models. *Proc. Natl. Acad. Sci. USA* **96**, 3228–3233.
- Hsiao, K., Chapman, P., Nilsen, S., Eckman, C., Harigaya, Y., Younkin, S., & Cole, G. (1996) Correlative memory deficits, A $\beta$  elevation, and amyloid plaques in transgenic mice. *Science* **274**, 99–102.
- Inestrosa, N. C., Alvarez, A., Pérez, C. A., Moreno, R. D., Vicente, M., Linker, C., Casanueva, O. I., Soto, C., & Garrido, J. (1996) Acetylcholinesterase accelerates assembly of amyloid- $\beta$ -peptides into Alzheimer's fibrils: Possible role of the peripheral site of the enzyme. *Neuron* **16**, 881–891.
- Irizarry, M. C., Soriano, F., McNamara, M., Page, K. J., Schenk, Games, D., & Hyman, B. T. (1997) A $\beta$  deposition is associated with neuropil changes, but not with overt neuronal loss in the human amyloid precursor protein V717F (PDAPP) transgenic mice. *J. Neurosci.* **17**, 7053–7059.
- Irizarry, M. C., McNamara, M., Fedorchak, K., Hsiao, K., & Hyman, B. T. (1997) APPsw Transgenic Mice develop age-related A $\beta$  deposits and neuropil abnormalities, but not neuronal loss in CA1. *J. Neuropathol. Exp. Neurol.* **56**, 965–973.
- Jucker, M., & Ingram, D. K. (1997) Murine models of brain aging and age-related neurodegenerative diseases. *Behav. Brain Res.* **85**, 1–25.
- Karnovsky, M. J., & Roots, L. (1964) A "direct coloring" thiocholine method for cholinesterases. *J. Histochem. Cytochem.* **12**, 219–221.
- Kitt, C. A., Höhmann, C., Coyle, J. T., & Price, D. L. (1994) Cholinergic innervation of mouse forebrain structures. *J. Comp. Neurol.* **341**, 117–129.
- Koliatsos, V. E., Price, D. L., Gouras, G. K., Cayouette M. H., Burton, L. E., & Winslow, J. W. (1994) Highly selective effect of nerve growth factor, brain-derived neurotrophic factor, and neurotrophin-3 on intact and injured basal forebrain magnocellular neurons. *J. Comp. Neurol.* **343**, 247–262.
- Kuhl, D. E., Minoshima, S., Fessler, J. A., Frey, K. A., Foster, N. L., Ficaró, E. P., Wieland, D. M., & Koeppe, R. A. (1996) *In vivo* mapping of cholinergic terminals in normal aging, Alzheimer's disease, and Parkinson's disease. *Ann. Neurol.* **40**, 399–410.

- McGeer, P. L., McGeer, E. G., Susuki, J., Dolman, C. E., & Nagai, T. (1984) Aging, Alzheimer's disease, and the cholinergic system of the basal forebrain. *Neurology* **34**, 741-745.
- Moechars, D., Dewachter, I., Lorent, K., Reversé, D., Baekelandt, V., Naidu, A., Tesseur, I., Spittaels, K., Van Den Haute, C., Cordell, B., Checler, F., Godaux, E., & Van Leuven, F. (1999) Early phenotypic changes in transgenic mice that overexpress different mutants of amyloid precursor protein in brain. *J. Biol. Chem.* **274**, 6483-6492.
- Moechars, D., Gilis, M., Kuipéri, C., Laenen, I., & Van Leuven, F. (1998) Aggressive behavior in transgenic mice expressing APP is alleviated by serotonergic drugs. *Neuroreport* **9**, 3561-3564.
- Moechars, D., Lorent, K., De Strooper, D., Dewachter, I., & Van Leuven, F. (1996) Expression in brain of amyloid precursor protein mutated in the  $\alpha$ -secretase site cause disturbed behavior, neuronal degeneration and premature death in transgenic mice. *EMBO. J.* **15**, 1265-1274.
- Morán, M. A., Mufson, E. J., & Gómez-Ramos, P. (1984) Colocalization of cholinesterases with  $\beta$  amyloid protein in aged and Alzheimer's brains. *Acta Neuropathol.* **85**, 362-369.
- Parnetti, L., Senin, U., & Mecocci, P. (1997) Cognitive enhancement therapy for Alzheimer's disease. *Drugs* **56**, 752-768.
- Pericak-Vance, M. A., & Haines, J. L. (1995) Genetic susceptibility to Alzheimer disease. *Trends Neurosci.* **11**, 504-508.
- Perry, E. K., Tomlinson, B. E., Blessed, G., Bergmann, K., Gibson, P. G., & Perry, R. H. (1978) Correlation of cholinergic abnormalities with senile plaques and mental test scores in senile dementia. *Br. Med. J.* **2**, 1457-1459.
- Price, D. L., Tanzi, R. E., Borchelt, D. R., & Sisodia, S. S. (1998) Alzheimer's disease: Genetic studies and transgenic models. *Annu. Rev. Genet.* **32**, 461-493.
- Procter, A. W. (1996) Neurochemical correlates of dementia. *Neurodegeneration* **5**, 403-407.
- Ransmayr, G., Cervera, P., Hirsch, E., Ruberg, M., Hersh, L. B., Duyckaerts, C., Hauw, J. J., Delumeau, C., & Agid, Y. (1989) Choline acetyltransferase-like immunoreactivity in the hippocampal formation of control subjects and patients with Alzheimer's disease. *Neuroscience* **32**, 701-714.
- Rodriguez-Puertas, R., Pascual, J., Vilaró, T., & Pazos, A. (1997) Autoradiographic distribution of M1, M2, M3 and M4 muscarinic receptor subtypes in Alzheimer's disease. *Synapse* **26**, 341-350.
- Rosenthal, H. E. (1967) A graphic method for the determination and representation of binding parameters in a complex system. *Anal. Biochem.* **20**, 525-532.
- Schenk, F., & Morris, R. G. M. (1985) Dissociation between components of spatial memory in rats after recovery from the effects of retrohippocampal lesions. *Exp. Brain. Res.* **58**, 11-28.
- Saper, C. B., German, D. C., & White, C. L. (1985) Neuronal pathology in the nucleus basalis and associated cell groups in senile dementia of the Alzheimer's type: Possible role in cell loss. *Neurology* **35**, 1089-1095.
- Sberna, G., Sáez-Valero, J., Li, Q. X., Czech, C., Beyreuther, K., Masters, C. L., McLean, C. A., & Small, D. H. (1998) Acetylcholinesterase is increased in the brains of transgenic mice expressing the C-terminal fragment (CT100) of the  $\beta$ -amyloid protein precursor of Alzheimer's disease. *J. Neurochem.* **71**, 723-731.
- Sharp, P. E., & Green, C. (1994) Spatial correlates of firing patterns of single cells in the subiculum of freely moving rat. *J. Neurosci.* **14**, 2339-2356.
- Stürchler-Pierrat, C., Abramowski, D., Duke, M., Wiederhold, K. H., Mistl, C., Rothacher, S., Ledermann, B., Burki, K., Frey, P., Paganetti, P. A., Waridel, C., Calhoun, M. E., Jucker, M., Probst, A., Staufenbiel, M., & Sommer, B. (1997) Two amyloid precursor protein transgenic mouse models with Alzheimer's disease-like pathology. *Proc. Natl. Acad. Sci. USA* **94**, 13287-13292.
- Tago, H., Kimura, H., & Maeda, T. (1986) Visualization of detailed acetylcholinesterase fiber and neuron staining in rat brain by sensitive histochemical procedure. *J. Histochem. Cytochem.* **34**, 1431-1438.
- Terry, R. D. (1996) The pathogenesis of Alzheimer disease: An alternative to the amyloid hypothesis. *J. Neuropathol. Exp. Neurol.* **55**, 1023-1025.
- Vogels, O. J. M., Broere, C. A. J., Ter Laak, H. J., Ten Donkelaar, H. J., Nieuwenhuys, R., & Schulte, B. P. M. (1990) Cell loss and shrinkage in the nucleus basalis of Meynert complex in Alzheimer's disease. *Neurobiol. Aging* **11**, 3-13.
- Whitehouse, P. J., Price, D., Clark, A. W., Coyle, J. T., & DeLong, M. R. (1981) Alzheimer Disease: Evidence for selective loss of cholinergic neurons in the nucleus basalis. *Ann. Neurol.* **10**, 122-126.
- Williams, L. R., Varon, S., Peterson, G. M., Victorin, K., Fisher, W., Bjorklund, A., & Gage, F. H. (1986) Continuous infusion of nerve growth factor prevents basal forebrain neuronal death after fimbria fornix transection. *Proc. Natl. Acad. Sci. USA* **83**, 9231-9235.
- Willson, C. A., & Hanin, I. (1995) Effect of nerve growth factor in ethylcholine mustard aziridinium (AF64A)-treated rats: Sensitization of cholinergic enzyme activity in the septohippocampal pathway. *J. Neurochem.* **65**, 856-862.
- Wong, T. P., Debeir, T., Duff, K., & Cuervo, A. C. Reorganization of cholinergic terminals in the cerebral cortex and hippocampus in transgenic mice carrying mutated presenilin-1 and amyloid precursor protein transgenes. *J. Neurosci.* **19**, 2706-2719.